The universal criterion for switching a magnetic vortex core in soft magnetic nanodots

Ki-Suk Lee[1], Sang-Koog Kim[1], Young-Sang Yu[1], Youn-Seok Choi[1], Konstantin Yu Guslienko[1], Hyunsung Jung[1], and Peter Fischer[2]

[1]Research Center for Spin Dynamics and Spin-Wave Devices, and Nanospinics Laboratory, Department of Materials Science and Engineering, College of Engineering, Seoul National University, Seoul 151-744 Republic of Korea

[2]Center for X-Ray Optics, Lawrence Berkeley National Laboratory, Berekeley, California 94720, USA

This work was supported by Creative Research Initiatives (ReC-SDSW) of MEST/KOSEF. P.F. was supported by the Director, Office of Science, Office of Basic Energy Sciences, of the U.S. Department of Energy under Contract No. DE-AC02-05CH11231.

The universal criterion for switching a magnetic vortex core in soft magnetic nanodots

Ki-Suk Lee,[1] Sang-Koog Kim,[1]* Young-Sang Yu,[1] Youn-Seok Choi,[1] Konstantin Yu Guslienko,[1] Hyunsung Jung,[1] and Peter Fischer[2]

[1]*Research Center for Spin Dynamics and Spin-Wave Devices, and Nanospinics Laboratory, Department of Materials Science and Engineering, College of Engineering, Seoul National University, Seoul 151-744, Republic of Korea*

[2]*Center for X-Ray Optics, Lawrence Berkeley National Laboratory, 1 Cyclotron Road, Mail Stop 2R0400, Berkeley, California 94720, USA*

The universal criterion for ultrafast vortex core switching between core-up and -down vortex bi-states in soft magnetic nanodots was empirically investigated by micromagnetic simulations and combined with an analytical approach. Vortex-core switching occurs whenever the velocity of vortex core motion reaches a critical value, which is $\upsilon_C = 330 \pm 37$ m/s for Permalloy, as estimated from numerical simulations. This critical velocity was found to be $\upsilon_C = \eta_C \gamma \sqrt{A_{ex}}$ with A_{ex} the exchange stiffness, γ the gyromagnetic ratio, and an estimated proportional constant $\eta_C = 1.66 \pm 0.18$. This criterion does neither depend on driving force parameters nor on the dimension or geometry of the magnetic specimen. The phase diagrams for the vortex core switching criterion and its switching time with respect to both the strength and angular frequency of circular rotating magnetic fields were derived, which offer practical guidance for implementing vortex core switching into future solid state information storage devices.

In magnetic thin films [1,2] and patterned magnetic elements of submicron (or smaller) size [3], a nontrivial spiral magnetization (**M**) configuration occurs and has been experimentally observed in both static and dynamic states. This magnetic nanostructure, the so-called "magnetic vortex" has an in-plane curling **M** along with an out-of-plane **M** at the core area stretching over of a few tens of nm in size [3]. Owing to a high thermal stability of this static structure [4] as well as the bi-state **M** orientations of the tiny vortex core (VC), the magnetic vortex has been received considerable attention as an information carrier of binary digits "0" and "1" in nonvolatile information storage technologies [4]. Furthermore, very recently, experimental, theoretical, and simulation studies have explored a rich variety of the dynamic properties of the magnetic vortex, including ultrafast VC switching by linearly oscillating [5-8] and circularly rotating [9-11] in-plane magnetic fields or spin-polarized currents [12,13], with extremely low-power consumption. The underlying mechanism and physical origin of ultrafast VC switching have also been found [8,14]. These rich dynamic properties stimulate continuing intensive studies of patterned nanodots in the vortex states targeting towards a fundamental understanding of their dynamics and real applications to a new class of nonvolatile random access memory and patterned information storage media. Such new conceptual devices using ultrafast, low-power VC switching becomes an emerging issue in the research areas of nanomagnetism and **M** dynamics.

Although, the fundamental understanding of VC reversal and vortex gyrotropic

motion dynamics has been much advanced recently, the universal criterion for VC switching, its phase diagram, and VC switching time still needs clarification. Moreover, these are technologically essential parameters for the manipulation of VCs, such as VC switching as basic component in future information storage devices.

In this Letter, we report that there is a critical velocity υ_C of the VC motion, which serves as the universal criterion required for VC switching, as found by micromagnetic simulations and analytical calculations. The constant value of υ_C only depends on the intrinsic material parameter of the exchange stiffness A_{ex} and does not vary with the dimension or geometry of a given nanodot as well as external driving force parameters. Based on the universality of υ_C we derive technologically useful phase diagrams of the VC reversal and the switching time with respect to the external force parameters.

In the present study, we chose as a micromagnetic simulation approach the OOMMF code [15] that utilizes the Landau-Lifshitz-Gilbert equation of motion [16] because this approach is a well established, optimized tool, and reliable enough to investigate **M** dynamics of vortex states of magnetic dots up to a few hundred nm in spatial and on the > 10 ps temporal scales. In addition, we used an analytical approach to determine the threshold of driving forces required for VC switching and the VC switching time with respect to external magnetic field parameters, based on the linearized Thiele equation [17] of motion of the VC position in the dot plane. We used Permalloy (Py) nanodots as a model system, each dot with

a different radius R ranging from 150 to 600 nm and a different thickness L ranging from 10 to 50 nm [see Fig. 1(a)].

To excite the vortex gyrotropic motion up to its VC switching, we used a specially designed driving force of counter-clockwise (CCW) circularly rotating magnetic fields in the film plane with the angular frequency ω_H and the strength H_0, denoted as $\mathbf{H}_{CCW} = H_0[\cos(\omega_H t)\hat{\mathbf{x}} + \sin(\omega_H t)\hat{\mathbf{y}}]$ [18]. The reason for selecting this CCW rotating field is that it is the eigenbasis and most efficient process for the resonantly excited eigenmotion of the core-up vortex state, as demonstrated in earlier theoretical and simulation [10,19], and experimental studies [11]. An example of the resonant vortex gyrotropic motion and VC switching driven by the CCW rotating field with a condition of H_0 = 20 Oe and $\nu_H = \omega_H/2\pi$ = $\omega_D/2\pi$ = 580 MHz (where $\nu_D = \omega_D/2\pi$ is the vortex eigenfrequency) [20,21] is represented by the orbital trajectories of the earlier transient and steady-state motions of the initial up core and its reversed down core along with their velocities following their individual orbital trajectories, as shown in Fig. 1(b). It is empirically found that the up-core switches to the down-core when the velocity of the up-core motion reaches a threshold velocity of v_C = 330 m/s for the Py dot [right panel in Fig. 1(b)].

To confirm the universality of this definite value of v_C = 330 m/s (see also Refs. [10,13,14]), we conducted additional simulations to obtain the VC velocity-versus-time curves versus both H_0 (10 to 350 Oe) and ν_H (0.1 to 2 GHz) for a Py dot of R = 150 nm

and L = 20 nm, as shown in Fig. 2(a). It is evident that the value of v_C = 330 ± 37 m/s is not affected by the external field parameters of ω_H and H_0, as well as the size of the Py dot, as evidenced by the independence of v_C on the dot size shown in Fig. 2(b). Furthermore, in order to examine the impact of intrinsic material parameters on the constant value of v_C = 330 ± 37 m/s, we performed simulations for a circular dot of a fixed geometry, namely R = 150 nm and L = 20 nm (artificially) varying the values of the saturation magnetization M_s, A_{ex}, and the gyromagnetic ratio γ, using $M_s/M_{s,Py}$ = 1.0 ~ 2.0, $(A_{ex}/A_{ex,Py})^{1/2}$ = 0.75 ~ 1.5, and γ/γ_{Py} = 0.5 ~ 1.75, where $M_{s,Py}$ = 860 G, $A_{ex,Py}$ = 1.3 μerg/cm, γ_{Py} = $2.8\times 2\pi$ MHz/Oe correspond to the values of Py. The simulation results in Figs. 2(c) and 2(d) display a linear increase of v_C with $(A_{ex}/A_{ex,Py})^{1/2}$ with an equal slope for different values of M_s, and a linear increase with γ/γ_{Py}, respectively.

All the simulation results lead to an explicit analytical form of $v_C \simeq \eta_C \gamma \sqrt{A_{ex}}$ with the proportional constant η_C, the value of which is estimated to be 1.66 ± 0.18 using just the simulation result of v_C = 330 ± 37 m/s for Py. It is interesting to note, that v_C is not determined by the other intrinsic parameter such as M_s. This fact can be understood from the physical origin of the VC switching. As reported previously [14], the VC gyrotropic motion driven by an external force induces the so-called gyrofield which originates from a dynamic deformation of **M** concentrated around the moving VC. This **M** deformation yields a large and spatially non-uniform excess effective field that acts against the **M** deformation, so that a

further **M** deformation suppresses the gyrofield. Thus, the resultant **M** deformation is determined by the balance between the gyrofield and the excess effective field. When the gyrofield reaches a sufficiently enough critical value to overcome the excess effective field, the resultant **M** deformation leads eventually to the VC switching via pure dynamic processes of the nucleation and annihilation of a vortex-antivortex pair [5-8]. Owing to the dramatic **M** deformation employed in a few nm area, the dominant contribution to the critical value of gyrofield is the short-range exchange field. Since the gyrofield is proportional to the VC velocity, A_{ex} is the dominant parameter in determining υ_C. Following the same argument, the long-range dipolar interaction is a negligible contribution to υ_C, so that the dimension and shape of a given dot, as well as M_s do not affect υ_C, as expressed in the form of $\upsilon_C \simeq \eta_C \gamma \sqrt{A_{ex}}$.

To summarize, υ_C only depends on A_{ex}, but neither geometry nor any driving force parameters such as ω_H and H_0. Consequently, one arrives at VC switching phase diagram and switching time diagram in the ω_H - H_0 plane. Figure 3 shows the simulation results on the criterion boundary diagram where VC switching (gray) and non-switching (white) areas are separated by different symbols for the several different dimensions of the Py dots, [R (nm), L (nm)] = [150, 20], [150, 30], [300, 20], and [450, 20]. The criterion boundaries for all different dimensions of the dots are found on almost the same line, which reflects again the fact that υ_C does not vary with the size of a given Py dot. Owing to the resonant excitation

of the VC motions at $\omega_{\mathrm{H}} = \omega_D$, the velocity can reach υ_C in VC motion even it is driven by only an extremely small field strength [5,10,11]. Resonant VC motions yield a valley in the criterion boundary in the vicinity of $\omega_{\mathrm{H}} = \omega_D$ and the threshold strength of H_0 required for VC switching is thus a minimum at $\omega_{\mathrm{H}} = \omega_D$.

In addition, we theoretically derived more general explicit analytical equations representing the criterion boundary which distinguishes the event of VC switching and non-switching based on the linearized Thiele's equation of motion. A detailed derivation is described in the supplementary online material [22]. Here we chose CCW rotating fields necessary for the up- to down-core switching [10,19]. From the general solution of VC motions in the linear regime, the velocity of the up-core motion driven by $\mathbf{H}_{\mathrm{CCW}}$ is written as

$$\upsilon(t) = \frac{\gamma R H_0}{3\sqrt{\left(\frac{G^2+D^2}{G^2} - \Omega\right)^2 + \frac{D^2}{G^2}\Omega^2}} \sqrt{\Omega^2 + F(\Omega, t)}, \qquad (1)$$

with the gyrovector $\mathbf{G} = -G\hat{\mathbf{z}}$, the diagonal damping tensor $\hat{D} = D\hat{I}$ with the identity matrix $\hat{I}$, the damping constant D, and $\Omega = \omega_{\mathrm{H}}/\omega_D$. The function $F(\Omega,t)$ represents the time variable velocity term of the transient VC motions. This explicit form also allows us to analytically construct the criterion boundary (RH_0^C) diagram of VC switching on the Ω-RH_0 plane, using Eq. (1) by setting $\upsilon = \upsilon_C = \eta_C \gamma \sqrt{A_{\mathrm{ex}}}$, as written by Eq. (2) below.

$$RH_0^C = \frac{3\upsilon_C}{\gamma} \sqrt{\frac{\left(\frac{G^2+D^2}{G^2} - \Omega\right)^2 + \frac{D^2}{G^2}\Omega^2}{\Omega^2 + F_M(\Omega)}}, \qquad (2)$$

where $F_M(\Omega)$ has the maximum at $t \approx \pi/|\omega_H - \omega_D|$. The numerical calculation of Eq.(2) using $\upsilon_C = 330 \pm 37$ m/s for Py estimated from simulations is displayed by the thick yellow region in Fig. 3. On resonance ($\Omega = 1$), the minimum value of RH_0^C is $3\left|\frac{D}{G}\right|(\upsilon_C/\gamma)$, where $\left|\frac{D}{G}\right| = \alpha\left[1.193 + \ln(R)/2 - \ln(L)/6 - \ln\left(\sqrt{2A}/M_s\right)/3\right]$ [23], indicating that $H_0^C \sim 3\left|\frac{D}{G}\right|(\upsilon_C/\gamma)/R$ at $\Omega = 1$ is the lowest field strength required for VC switching [24]. The analytical solution (thick yellow region) is somewhat in discrepancy with the micromagnetic simulations (symbols), although they are similar in shape/trend. This discrepancy can be associated with the fact that the present simulations of VC switching imply a nonlinearity of VC gyrotropic motions near its switching event [25], whereas Eq. (2) assumes only linear-regime vortex motions. However, this nonlinear effect could be compensated by multiplying a scaling factor S_F = + 1.4 to Eq. (2) that was derived based on the linearized Thiele's equation of the vortex motion. Recent experimental results by Curcic *et al.* [11] support well our results. They reported $H_0^C = 3.4$ Oe and $\upsilon_C = 190$ m/s for a square dot of 500 width and 50 nm thickness, being in quite good agreement with our estimated value of $H_0^C = 4.1$ Oe from $\left[3\left|\frac{D}{G}\right|(\upsilon_C/\gamma)/R\right] \cdot S_F$ on resonance for the assumption of R = 250 nm, $\upsilon_C = 190$ m/s, and the scaling factor $S_F = 1.4$.

Using Eq. (1), the diagram for the switching time t_s, i.e., the time when the VC switching is completed (or upon υ reaches υ_C) was numerically calculated with respect to both ω_H and H_0. For the resonance case $\Omega = 1$, t_s is analytically expressed as

$t_S = \left(\frac{G^2+D^2}{\kappa D}\right)\ln\left[1-\left(H_0^C/H_0\right)\right]$ for $H_0 > H_0^C$ (non-switching for $H_0 < H_0^C$). For all the cases of $\Omega \neq 1$, t_s can be numerically calculated by putting $\upsilon = \upsilon_C$ from Eq. (1) along with the correction of the nonlinear effect of VC switching, as shown in Fig. 4(a), for example, for a Py dot of R= 150 nm and L= 20 nm. For the cases of $H_0 \gg H_0^C$, t_s is ~ 1 ps, and does not much vary with ω_{H}, but as H_0 decreases close to H_0^C, t_s markedly increases and varies with ω_{H}. At $\Omega = 1$, it appears that the lower H_0^C, the longer t_s [26]. For faster VC switching, larger values of H_0 and $\omega_{\mathrm{H}} > \omega_D$ are more effective. For $\omega_{\mathrm{H}}/\omega_D$ = 0.6, 1.0, and 1.6, those corresponding t_s-versus-H_0 curves were plotted along with the simulation results (symbols) [Fig. 4(b)], both being in good agreement. It should be pointed out, that the switching time diagram will be technologically useful in the optimization of driving force parameters that reliably control ultrafast VC switching. Note that this switching is a pure dynamical process, which does not involve overcoming any energy barriers as in the classical Neel-Brown case [1].

In conclusion, by conducting micromagnetic simulations and analytical calculations we have found that the universal criterion for vortex core switching is the critical velocity of vortex-core gyrotropic motion, which is expressed as $\upsilon_C = \eta_C \gamma \sqrt{A_{\mathrm{ex}}}$ with $\eta_C = 1.66 \pm 0.18$, and exhibits a constant value of $\upsilon_C = 330 \pm 37$ m/s for Py. From this criterion, the VC switching diagram and switching time diagram for VC switching with respect to the driving force parameters were constructed, which will provide guidance for practical

implementations of an array of dots in vortex state to information storage devices in terms of information storage, writing, and reading operations. They are also technologically useful in the design of the dot dimensions and proper choice of materials as well as to optimize external driving forces for reliable ultrafast VC switching at extremely low power consumption.

This work was supported by Creative Research Initiatives (ReC-SDSW) of MEST/KOSEF. P.F was supported by the Director, Office of Science, Office of Basic Energy Sciences, Materials Sciences and Engineering Division, of the U.S. Department of Energy.

References

* To whom all correspondence should be addressed: sangkoog@snu.ac.kr

[1] A. Hubert, and R. Schäfer, *Magnetic Domains* (Springer-Verlag, Berlin, New York, Heidelberg, 1998).

[2] S.-K. Kim, J. B. Kortright, and S.-C. Shin, Appl. Phys. Lett. **78**, 2742 (2001); S.-K. Kim *et al.*, Appl. Phys. Lett. **86**, 052504 (2005).

[3] T. Shinjo *et al.*, Science **289**, 930 (2000); A. Wachowiak *et al.*, Science **298**, 577 (2002).

[4] R. P. Cowburn, Nature Mater. **6**, 255 (2007); J. Thomas, Nature Nanotech. **2**, 206 (2007).

[5] B. Van Waeyenberge *et al.*, Nature **444**, 461 (2006).

[6] R. Hertel, S. Gliga, M. Fähnle, and C. M. Schneider, Phys. Rev. Lett. **98**, 117201 (2007).

[7] Q. F. Xiao *et al.*, J. Appl. Phys. **102**, 103904 (2006).

[8] K.-S Lee, K. Y. Guslienko, J.-Y. Lee, and S.-K. Kim, Phys. Rev. B **76**, 174410 (2007).

[9] V. P. Kravchuk *et al.*, J. Appl. Phys. **102**, 043908 (2007).

[10] S.-K. Kim, K.-S. Lee, Y.-S. Yu, and Y.-S. Choi, Appl. Phys. Lett. **92**, 022509 (2008).

[11] M. Curcic *et al.*, e-print arXiv:cond-mat/0804.2944v2.

[12] K. Yamada *et al.*, Nature Mater. **6**, 269 (2007).

[13] S.-K. Kim *et al.*, Appl. Phys. Lett. **91**, 082506 (2007).

[14] K. Y. Guslienko, K.-S. Lee, and S.-K. Kim, Phys. Rev. Lett. **100**, 027203 (2008).

[15] See http://math.nist.gov/oommf.

[16] L. D. Landau and E. M. Lifshitz, Phys. Z. Sowjet. **8**, 153 (1935); T. L. Gilbert, Phys. Rev. **100**, 1243 (1955).

[17] A. A. Thiele, Phys. Rev. Lett. **30**, 230 (1973); D. L. Huber, Phys. Rev. B **26**, 3758 (1982).

[18] A linearly oscillating field can be decomposed into the CCW and CW rotating fields with the same H_0 and ω_H [10].

[19] K.-S. Lee and S.-K. Kim, Phys. Rev. B **78**, 014405 (2008).

[20] K. Y. Guslienko *et al.*, J. Appl. Phys. **91**, 8037 (2002).

[21] J. P. Park *et al.*, Phys. Rev. B **67**, 020403(R) (2003); S. B. Choe *et al.*, Science **304**, 420 (2004); K. Y. Guslienko *et al.*, Phys. Rev. Lett. **96**, 067205 (2006).

[22] See EPAPS Document No. XXX for detailed descriptions. For more information on

EPAPS, see http://www.aip.org/pubservs/epaps.html.

[23] K. Y. Guslienko, Appl. Phys. Lett **89**, 022510 (2006).

[24] For the CW rotational field, RH_0^C has the constant value of $3\upsilon_C/\gamma$ which indicate $RH_0^C \gg RH_0^C$ for p = +1. Very recently, these asymmetric switching behaviors has been verified experimentally [11].

[25] K.-S. Lee and S.-K. Kim, Appl. Phys. Lett **91**, 132511(2007); K. S. Buchanan *et al.*, Phys. Rev. Lett. **99**, 267201 (2007).

[26] From the results of micromagnetic simulation for the 150 nm (300 nm) radius and 20 nm thickness Py nanodot, the minimum field amplitude required for VC switching is only 14 Oe (7 Oe) whereas the switching time is 17 ns (33 ns).

FIG. 1 (color online). (a) Magnetic vortex structure with either upward or downward core **M** orientation. The rotation sense of the local in-plane **M**s around the VC is counter-clockwise (CCW). (b) Orbital trajectories (left) and velocity-versus-time curve of the up (red line) and down (blue line) cores in a circular Py nanodot of R = 150 nm and L = 20 nm driven by the indicated CCW rotating field $\mathbf{H}_{\mathrm{CCW}}$ (inset) with $\omega_{\mathbf{H}} / \omega_D$ = 1 and H_0 = 20 Oe. The horizontal line (right) denotes the value of υ_C = 330 m/s with an estimated error value of ● 37 m/s (gray-color region)

FIG. 2 (color online). (a) VC velocity υ in the Py dot of R = 150 nm and L = 20 nm for different values of H_0 and $\Omega = \omega_{\mathbf{H}} / \omega_D$ of the $\mathbf{H}_{\mathrm{CCW}}$. (b), (c), and (d) show the dependence of υ_C on the dimensions of the Py dot, the material parameters of A_{ex} and M_{s}, and γ, respectively. All the results were obtained from micromagnetic numerical simulations. The gray-colored region with the line indicates the critical velocity with its error range.

FIG. 3 (color online). Criterion boundary diagram of VC switching driven by $\mathbf{H}_{\mathrm{CCW}}$ with respect to the $\Omega - RH_0$ plane. Blue circle, green triangle, orange square, black diamond symbols correspond to the micromagnetic simulation results with [R (nm), L (nm)] = [150, 20], [150, 30], [300, 20], [600, 20], respectively. Yellow colored area indicates the criterion boundary obtained using the analytical Eq. (2) for Py dots with R = 50 ~ 5000 nm and L = 20

~ 80 nm, based on the estimated value of $\upsilon_C = 330 \pm 37$ m/s for Py. The light purple colored area is the result of the multiplication of 1.4 to Eq. (2) (yellow colored area). The blue colored axis indicates the results corresponding to a specific Py dot of [R (nm), L (nm)] = [150, 20].

FIG. 4 (color online). (a) Contour plot of VC switching time t_s on the $\omega_H - H_0$ plane for the Py dot with R = 150 nm and L = 20 nm. (b) t_s-versus-H_0 curves for specific values of ω_H / ω_D = 0.6, 1.0, and 1.6, along with the corresponding simulation results.

FIG.1

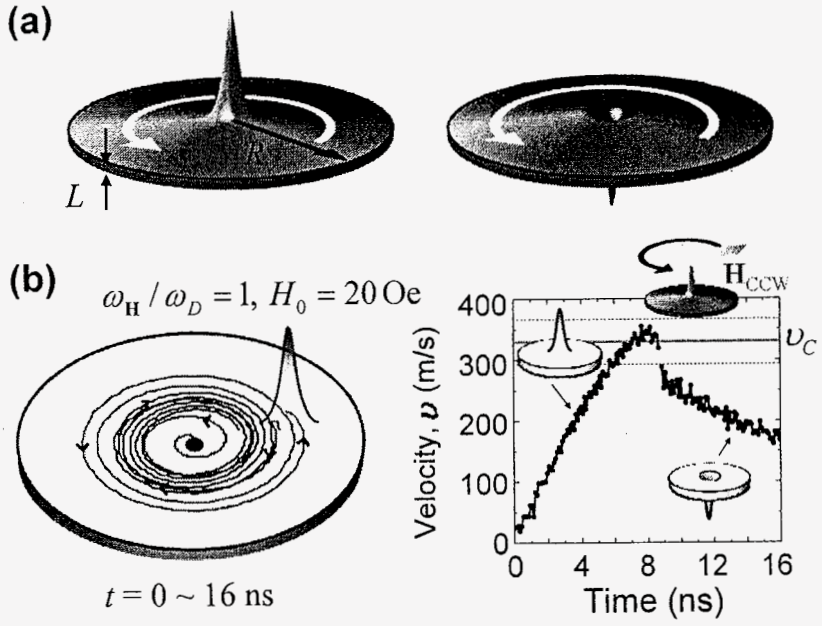
(a)
L
(b)
$\omega_H / \omega_D = 1,\ H_0 = 20\,\mathrm{Oe}$
$t = 0 \sim 16$ ns
H_{CCW}
v_C
Velocity, v (m/s)
400
300
200
100
0
0
4
8
12
16
Time (ns)

FIG.2

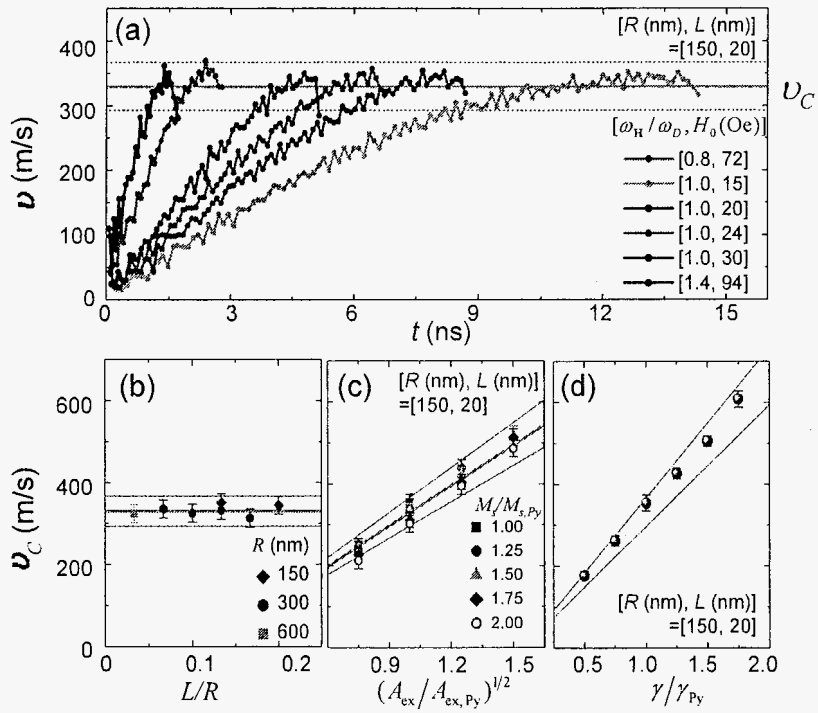
(a)
[R (nm), L (nm)]
=[150, 20]
υ_C
$[\omega_H/\omega_D, H_0(\mathrm{Oe})]$
[0.8, 72]
[1.0, 15]
[1.0, 20]
[1.0, 24]
[1.0, 30]
[1.4, 94]
υ (m/s)
t (ns)
(b)
(c)
(d)
υ_C (m/s)
R (nm)
150
300
600
L/R
$M_s/M_{s,Py}$
1.00
1.25
1.50
1.75
2.00
$(A_{ex}/A_{ex,Py})^{1/2}$
γ/γ_{Py}

FIG.3

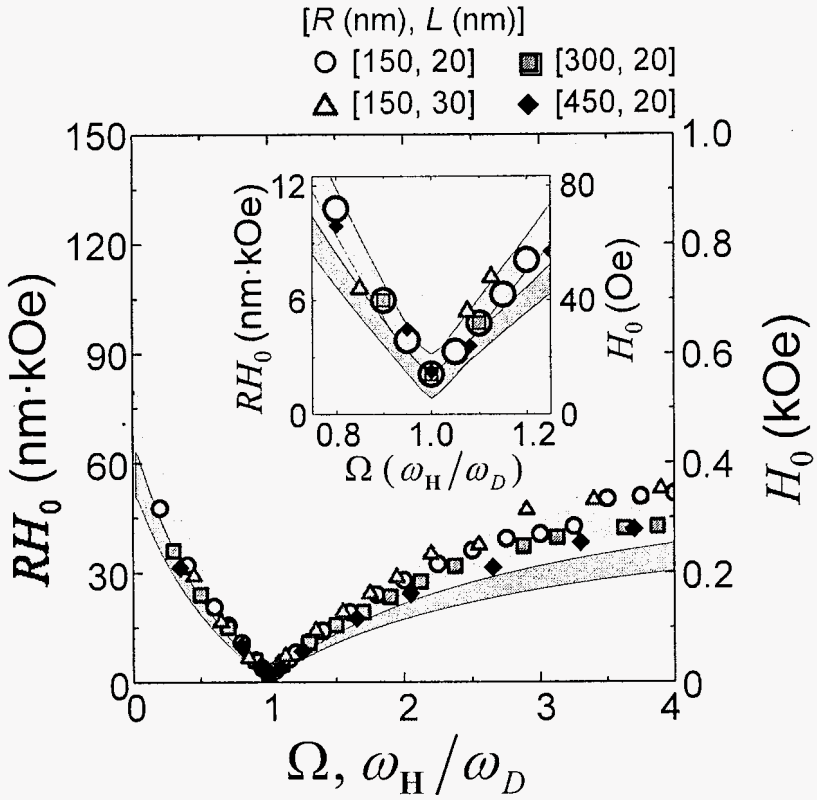
[R (nm), L (nm)]
[150, 20]
[300, 20]
[150, 30]
[450, 20]
RH_0 (nm·kOe)
H_0 (kOe)
Ω, ω_H/ω_D
RH_0 (nm·kOe)
H_0 (Oe)
Ω (ω_H/ω_D)

FIG.4

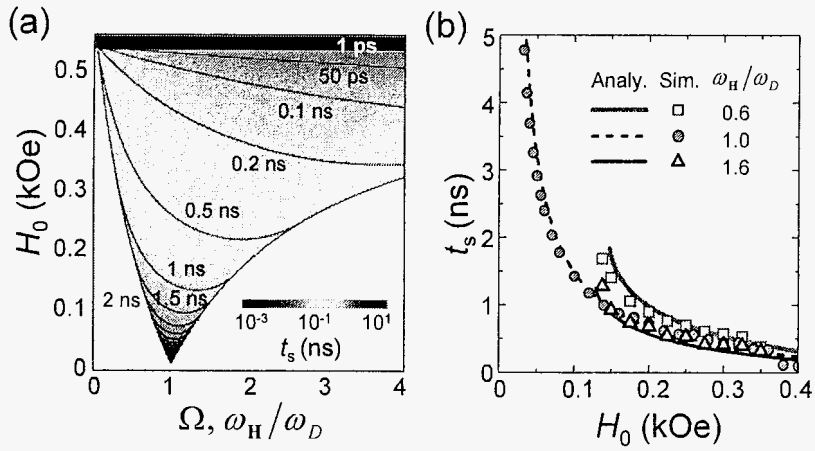
(a)
1 ps
50 ps
0.1 ns
0.2 ns
0.5 ns
1 ns
1.5 ns
2 ns
10^{-3} 10^{-1} 10^{1}
t_s (ns)
H_0 (kOe)
$\Omega, \omega_H/\omega_D$
(b)
Analy. Sim. ω_H/ω_D
0.6
1.0
1.6
t_s (ns)
H_0 (kOe)

Supplementary Documents

Derivation of Eq. (1)

To obtain the velocity of VC motions in the linear regime, we derived the general solution of VC motions including the earlier transient and later steady state motions [1] based on the linearized Thiele's equation [2] for the VC position $\mathbf{X} = (X, Y)$: $-\mathbf{G}\times\dot{\mathbf{X}} - \hat{D}\dot{\mathbf{X}} + \partial W(\mathbf{X},t)/\partial\mathbf{X} = 0$ with the gyrovector $\mathbf{G} = -G\hat{\mathbf{z}}$, and the damping tensor $\hat{D} = D\hat{I}$ with the identity matrix $\hat{I}$, the damping constant D and the potential energy function $W(\mathbf{X},t)$ [1,3]. To solve elementary rotating eigenmotions of a VC in a circular dot driven by the CCW- and CW- circular rotating fields [4,5], it is useful to describe the VC position using a complex variable $S \equiv X + iY$ where the real and imaginary values indicate the x- and y-positions of the VC, respectively. For the case of $\mathbf{H}_{\mathrm{CCW}}$ for a selective switching from the up- to down-core, the general solution in the linear regime is given as $S = [S(0) - S_0]\exp(i\omega_D t)\exp(\omega_D D t/|G|) + S_0\exp(i\omega_{\mathrm{H}} t)$ [6] with $\omega_D = \kappa|G|/(G^2 + D^2)$ [7] where κ is the stiffness coefficient of the potential energy $W(S,t)$, $S_0 = i\mu H_0/(\kappa - \omega_{\mathrm{H}}G - i\omega_{\mathrm{H}}D)$, and $S(0) = X_0 + iY_0$. $\mathbf{X}(0) = (X_0, Y_0)$ is the VC position at $t = 0$. From the time derivation of this general solution, the velocity of the up core motion driven by $\mathbf{H}_{\mathrm{CCW}}$ is written as

$$\upsilon(t) = \frac{\gamma R H_0}{3\sqrt{\left(\frac{G^2+D^2}{G^2} - \Omega\right)^2 + \frac{D^2}{G^2}\Omega^2}} \sqrt{\Omega^2 + F(\Omega,t)}, \qquad (1)$$

with the transient term

$$F(\Omega,t) = \frac{G^2+D^2}{G^2}\exp\left(2\frac{D\omega_D t}{|G|}\right) - 2\Omega\exp\left(\frac{D\omega_D t}{|G|}\right)\left[\cos\left((1-\Omega)\omega_D t\right) + \frac{D}{|G|}\left[\sin\left((1-\Omega)\omega_D t\right)\right]\right]$$

, where $\Omega = \omega_H/\omega_D$. For a sufficiently large value of t, the function $F(\Omega,t)$ converges to 0, i.e., the vortex motion arrives at a pure steady state (the earlier transient state disappears). The vortex motion becomes a steady-state motion (non time dependence), thus its velocity turns into $\upsilon = \frac{\gamma R H_0}{3\sqrt{\left(\frac{G^2+D^2}{G^2} - \Omega\right)^2 + \frac{D^2}{G^2}\Omega^2}}\Omega$.

References

[1] K.-S. Lee and S.-K. Kim, Appl. Phys. Lett. **91**, 132511 (2007).

[2] A. A. Thiele, Phys. Rev. Lett. **30**, 230 (1973); D. L. Huber, Phys. Rev. B **26**, 3758 (1982).

[3] K. Y. Guslienko, V. Novosad, Y. Otani, H. Shima, and K. Fukamichi, Phys. Rev. B **65**, 024414 (2002); K. Y. Guslienko, Appl. Phys. Lett. **89**, 022510 (2006).

[4] K.-S. Lee and S.-K. Kim, Phys. Rev. B **78**, 014405 (2008).

[5] S.-K. Kim, K.-S. Lee, Y.-S. Yu, and Y.-S. Choi, Appl. Phys. Lett. **92**, 022509 (2008).

[6] K.-S. Lee and S.-K. Kim (unpublished).

[7] S.-K. Kim, Y.-S. Choi, K.-S. Lee, K. Y. Guslienko, and D.-E. Jeong, Appl. Phys. Lett. **91**, 082506 (2007).